Geoderma 406 (2022) 115466

Contents lists available at ScienceDirect

Geoderma

journal homepage: www.elsevier.com/locate/geoderma

Linkages between soil organic matter and magnetic mineral formation in agricultural fields in southeastern Minnesota, USA

Aaron L. Frankl [a,b,*], Daniel P. Maxbauer [a], Mary E. Savina [a]

[a] Department of Geology, Carleton College, Northfield, MN 55057, United States
[b] Deparment of Soil, Water, and Climate, University of Minnesota, St. Paul, MN 55108, United States

ARTICLE INFO

Handling Editor: Cristine L.S. Morgan

Keywords:
Soil magnetism
Soil organic matter
Environmental magnetism

ABSTRACT

Magnetic properties of soil are widely utilized to study soil development in a variety of settings due to the formation of strongly magnetic iron oxides during pedogenesis. Similarly, soil organic matter (SOM) is commonly measured in soil surveys conducted on agricultural lands due to the essential role SOM plays in the soil ecosystem. Here, we present data from two agricultural fields in southeastern Minnesota that demonstrate a relationship between soil magnetic properties and SOM. In each field, we collected 100 topsoil samples along a 40 m by 20 m grid to determine spatial variability in soil magnetic properties and SOM, as well as two soil cores to constrain variability with depth (~0–60 cm). Magnetic susceptibility, low-field remanence, and hysteresis properties were used to characterize magnetic mineral abundance and grain-size in the soils. There are strong positive correlations between SOM and three magnetic properties: the frequency dependence of susceptibility (χ_{fd}), anhysteretic remanent magnetization (ARM), and the ratio of ARM to isothermal remanent magnetization (ARM/IRM). All three of these magnetic properties (χ_{fd}, ARM, and ARM/IRM) are sensitive to the concentration (or relative abundance) of fine-grained (<75 nm) magnetite/maghemite known to form in well-drained soils during pedogenesis. Correlation between SOM and magnetic properties persist in each field despite differences in the management strategy over the past three decades. Our results support a functional link between SOM and soil-formed magnetite/maghemite, where increasing SOM (up to a threshold) enhances the production and stability of soil-formed magnetite due to its role in soil redox processes and iron-organic complexes. Agricultural soils seem particularly well suited to demonstrate correlations between SOM and pedogenic magnetic minerals due to their relatively low SOM and typically well-drained environments, supporting the utility of soil magnetism in agricultural soil survey studies.

1. Introduction

The magnetic properties of soils are a longstanding area of interest (Le Borgne, 1955; Le Borgne, 1960) and represent a relatively low-cost means for characterizing the composition, abundance, and grain size of various iron oxide minerals in soil. Applications of soil magnetism are varied and range from studies aimed at monitoring spatial distribution of pollutants (e.g., Blundell et al., 2009a; Camargo et al., 2018; Hanesch and Scholger, 2002; Liu et al., 2012) to the reconstruction of past climates (e.g., Geiss et al., 2008; Jordanova and Jordanova, 2021; Maher, 1998; Maxbauer et al., 2016). However, to date, relatively few researchers have studied soil magnetism in agricultural systems (see Pingguo et al., 2016; Yang et al., 2015 for two recent examples).

Several studies identify a relationship between magnetic properties and soil organic matter (SOM) in non-agricultural settings (Blundell et al., 2009b; César de Mello et al., 2020; Dearing et al., 1996; Jakšík et al., 2016; Jordanova, 2016; Maher, 1998; Neumeister and Peschel, 1968; Quijano et al., 2014). Correlation between SOM and soil magnetic properties in these studies are usually attributed to climate and other soil forming factors that control both properties similarly (Maher, 2016). SOM in agricultural settings is dynamically impacted by many non-natural soil forming factors related to land-use (for example, tillage practices) and varies considerably in agricultural areas experiencing uniform climate (Fan et al., 2020; Ferreira et al., 2016; Huang et al., 2007). Given that SOM is a key indicator of agricultural soil quality (Larkin, 2015; Marchetti et al., 2012) and impacts many physical, chemical, and biological properties and functions in soil (Cannell and Hawes, 1994; Dalal et al., 2003; Franzluebbers, 2002; Rawls et al., 2003;

* Corresponding author at: Borlaug Hall, 1991 Upper Buford Cir, St. Paul, MN 55108, United States.
E-mail address: fran1361@umn.edu (A.L. Frankl).

https://doi.org/10.1016/j.geoderma.2021.115466
Received 26 March 2021; Received in revised form 10 September 2021; Accepted 12 September 2021
Available online 27 September 2021

Reeves, 1997), a better understanding of the relationship between magnetic properties and SOM within agricultural soils will help improve our understanding of this linkage in systems where climate cannot play a role in the relationship.

Here, we explore variation in SOM and soil magnetic properties in two adjacent agricultural fields in southeastern Minnesota. Despite differences in land management practices described below, both fields are generally well-drained, have relatively flat topography, similar parent material, and experience the same climate. We hypothesize, then, that any correlations between magnetic properties and SOM ought to be related to pedogenic processes that directly link SOM to the production of pedogenic iron oxides. We propose a modification to a well-known model for magnetic enhancement where coupled SOM oxidation and iron reduction leads to the production of nanoscale magnetite (Fe_3O_4; Lovley, 1987; Orgeira et al., 2011). This model is well-known amongst the environmental magnetic community, where the magnetic enhancement of soil is useful in the reconstruction of past climate (see reviews in Ahmed and Maher, 2018; Evans and Heller, 2003; Liu et al., 2012; Maher, 1998, 2007, 2011; Maxbauer et al., 2016; Mullins, 1977; Orgeira et al., 2011; Thompson and Oldfield, 1986). Here, we emphasize that this mechanistic relationship between SOM and pedogenic magnetite may be particularly relevant in agricultural fields, where soil magnetism is less well studied.

1.1. Site background

Study sites are located just northwest of Northfield, Minnesota in the southwest corner of Dakota County (Fig. 1). Soils in this area develop on a thin layer of loess atop loamy glacial till deposited by the Des Moines Lobe of the Laurentide Ice Sheet ~12,000–14,000 years ago (Hobbs et al., 1990). Prior to European settlement (~1850), native vegetation in the area was a mixture of prairie and hardwood forests that produced heterogeneous soil characteristics at the study site (United States Department of Agriculture, 1983). The study areas contain a mixture of soil series assigned as either Mollisols and Alfisols (see Fig. S1; (Soil Survey Staff, 2020). Plowing has homogenized much of the A and upper B horizons on both farms. Climate in Dakota County is subhumid and characteristically has large temperature variations between summer and winter (United States Department of Agriculture, 1983). The mean annual temperature is 6.9 °C with an average temperature of −8.9 °C and 21.1 °C in the winter and summer, respectively (United States Department of Agriculture, 1983). During winter, soils freeze to a depth of approximately 2 to 3 m. The average annual precipitation is 77.8 cm (National Weather Service Forecast Office, 2019). The area has

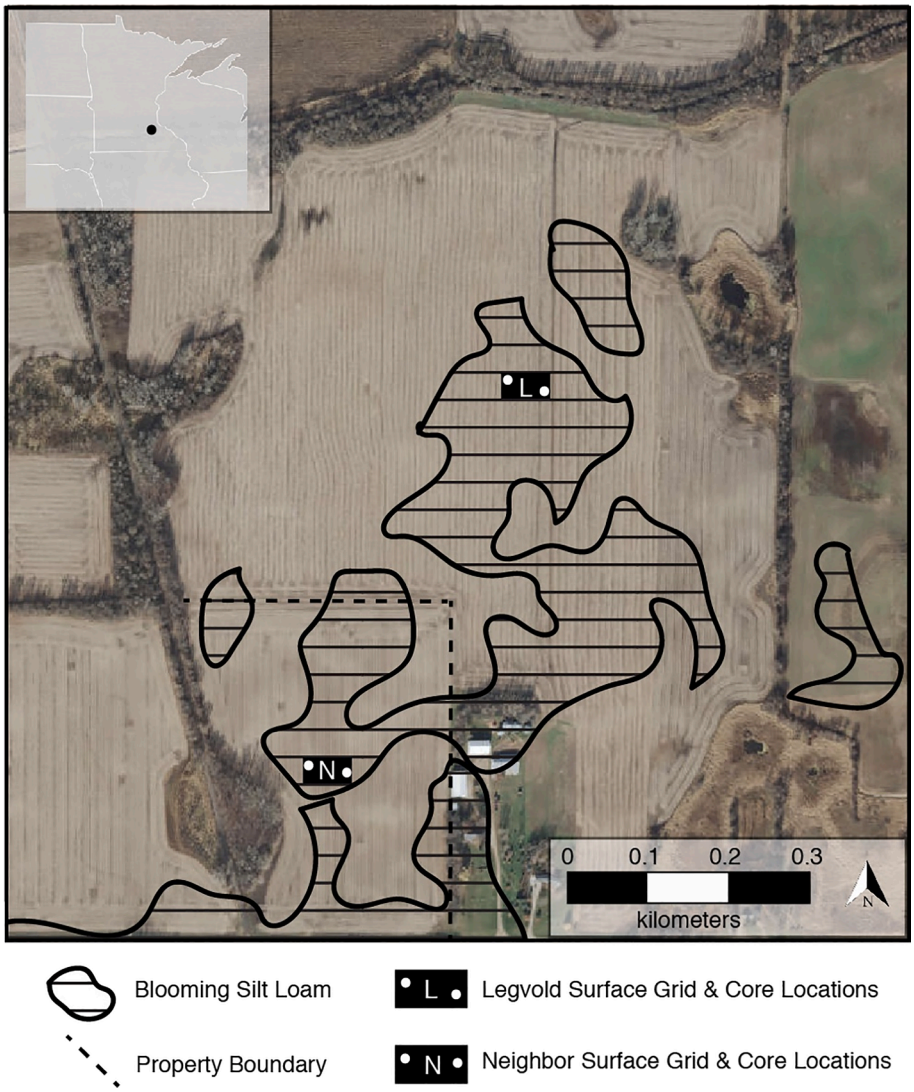

Fig. 1. Location of sample collection sites in Northfield, Minnesota. L and N indicate the 40 m × 20 m grids where 100 topsoil samples were collected on the Legvold Farm and the Neighbor Farms, respectively. The patterned area represents the mapped extent of the Blooming soil series on both farms (from the USDA's Web Soil Survey). All samples (topsoil, cores) were collected from areas mapped as the Blooming soil series. Image from Google Earth (November 2015).

experienced particularly thick snowpacks and increased precipitation in the past decade, including during the year of study (109.7 cm of precipitation; National Weather Service Forecast Office, 2019). Increased precipitation during the past few years has produced irregularities in harvest dates and placed significant strain on agricultural drainage systems.

We report data from two fields, referred to throughout this study as the Legvold Farm and Neighbor Farm. There is a long history of research at the Legvold Farm, including a comparative agroecosystem study which examined the effects of tillage and cropping patterns on the ecology of different farms (Gregory et al., 2005). In addition, several unpublished undergraduate projects from students at nearby Carleton College and St. Olaf College contribute to knowledge of the geologic and biological context for the site. Between 1879 and 1916 much of the 110-acre Legvold Farm was cleared of both trees and swampy land (some patches of marsh, as well as small, filled-in depressions, remain). Since 1991, the Legvold Farm has utilized strip-till farming with annual corn-soybean rotation and cover crops during the winter. An original concrete tiling system was installed around 1960, but likely degraded over time and was ineffective by the early 2000s. A modern, plastic tiling system was established between 2006 and 2008 (these dates were derived from interpretations of aerial imagery); additionally, a controlled drainage structure and a saturated buffer were installed in 2015 along the field's northern edge to regulate subsurface soil moisture and reduce nutrient pollution. At the time of sampling, the Legvold Farm had standing soybean crop.

The Neighbor Farm is located directly to the west of the Legvold Farm fields (Fig. 1) and there is no known previous research from this site. Between 1957 and 1964 the Neighbor fields were cleared for agriculture (Fig. S2). To our knowledge, the Neighbor Farm has only been conventionally tilled with either corn-soybean or corn-on-corn crop rotation. In contrast to the Legvold Farm, the Neighbor Farm is naturally well-drained and does not utilize tile drainage on its 40 acres. Due to changes in ownership, land management practices at the Neighbor Farm will be shifting, and at the time of sampling, the field had a standing alfalfa cover crop.

1.1.1. Blooming silt loam

Despite soil heterogeneity in the area and across the full acreage of the studied fields, all soils sampled here are mapped as the Blooming silt loam (Fine-loamy, mixed, superactive, mesic Mollic Hapludalfs; referred to as simply Blooming or Blooming series in this paper), as defined by the USDA's Web Soil Survey (Soil Survey Staff, 2020). The Blooming is typically a silt loam, formed from silty and loamy sediments (likely derived from loess) overlying glacial till; the Blooming is well-drained. Native vegetation of the Blooming series is primarily deciduous forest (Soil Survey Staff, 2006). Soybean and corn are the most common cultivated crops on the Blooming series (Soil Survey Staff, 2006). The Blooming Series is found in Central and Northern Iowa, and in Southeast Minnesota (Soil Survey Staff, 2006).

The typical Blooming Series pedon has an Ap (plowed) horizon which extends to 20 cm depth, and is very dark brown to black in color, and a silt loam in texture (Fig. S3; Soil Survey Staff, 2006). Below the Ap horizon is a brown, silt loam BE horizon, which extends to approximately 38 cm depth. Four Bt horizons totaling 84 cm thickness, underlie the BE; these horizons are developed on glacial till, contain rock fragments, and have loam to sandy clay loam textures (with clay films), which extend past one meter depth. The colors of the Bt horizons vary from brown to yellow and olive browns (Soil Survey Staff, 2006). A loamy C horizon extends to the glacial till parent material, at 152 cm depth. The soils in the study area are similar to the type pedon of the Blooming series, which is located in Steele County, MN ~72 km south of our study site, except that there is no BE horizon, so the Ap horizon rests directly over the Bt.

2. Materials and methods

2.1. Sampling and sample preparation

In each field, 100 topsoil samples were collected in a 40 m by 20 m grid (Fig. 2). Both grids were established in areas mapped as Blooming series. It is important to note that the Web Soil Survey soil mapping units are heterogenous, and that projections of the Blooming series also consist of 10% Merton silt loam (Fine-loamy, mixed, superactive, mesic Aquic Hapludolls). The grids share the same parent material (silty sediments over glacial till) and climate. Although the grid areas are not entirely flat, topographic irregularities are too small in scale to be shown at one-meter resolution DEM from available LiDAR data. Major differences in the soil characteristics between the two study grids likely derive from anthropogenic changes and land management practices noted above (and discussed in more detail in our discussion).

Topsoil samples were collected using an auger from a depth of 10–25 cm (sampled from homogenous Ap horizons). Samples were taken from within soil peds to minimize auger contamination. In both fields, the upper soil (0–25 cm depth) has been homogenized due to plowing. As a result, any subtle differences in our sampling depth are unlikely to have influenced the results. Two one-meter soil cores were acquired from each site and sampled in 5–10 cm intervals to a depth of 60 cm using a slide-hammer coring device and auger. A total of 19 samples were taken from these deeper cores at the Legvold Farm cores and 14 from cores on the Neighbor Farm.

2.2. Sample preparation

Soil samples for magnetic analyses were dried, lightly crushed to homogenize, and sieved to remove large inorganic particles and any organic fragments>1 mm. We note that 2 mm is more typical in soil studies, however our focus for magnetic measurements is on fine-grained particles generally less than 150 nm so the choice of a finer sieve size does not appreciably impact our results. From each homogenized sample, a specimen was packed into a diamagnetic plastic cube and secured with a non-magnetic potassium silicate adhesive for magnetic analyses. Samples analyzed for SOM via loss-on-ignition (LOI), were homogenized and lightly crushed, but not sieved (although any large root fragments were removed by hand).

2.3. Loss-on-ignition

LOI is a common technique used to quantify the weight percent organic matter in soil and other sediments (e.g., Dean, 1974; Heiri et al., 2001; Santisteban et al., 2004; Soil Survey Staff, 2014). Homogenized soil samples were placed in weighed crucibles and weighed again before two heating treatments. First, water loss was determined from weight loss after heating to 100 °C for 12 h. To measure organic content, weight loss was measured again after heating the samples at 550 ℃ for 4 h. Crucibles were cooled completely before weighing. The weight percent SOM was calculated for each sample as, SOM = [weight following 550 ℃ heating] / [weight following 100℃ heating to remove water content] × 100. LOI analyses were conducted at the National Lacustrine Core Facility (LacCore) at the University of Minnesota.

2.4. Magnetic measurements

For each specimen in this study (n = 200 topsoil, n = 33 from soil cores), the mass-normalized magnetic susceptibility (χ, m^3kg^{-1}) at low (465 Hz) and high (4650 Hz) frequencies was measured using a Magnon variable frequency susceptibility meter in an alternating current (AC) field of 300 Am^{-1}. The χ values used in our analyses represent the average of four replicate measurements at each frequency for each specimen. Magnetic susceptibility measures the total contribution of all mineral constituents present in a soil to its magnetism; these can include

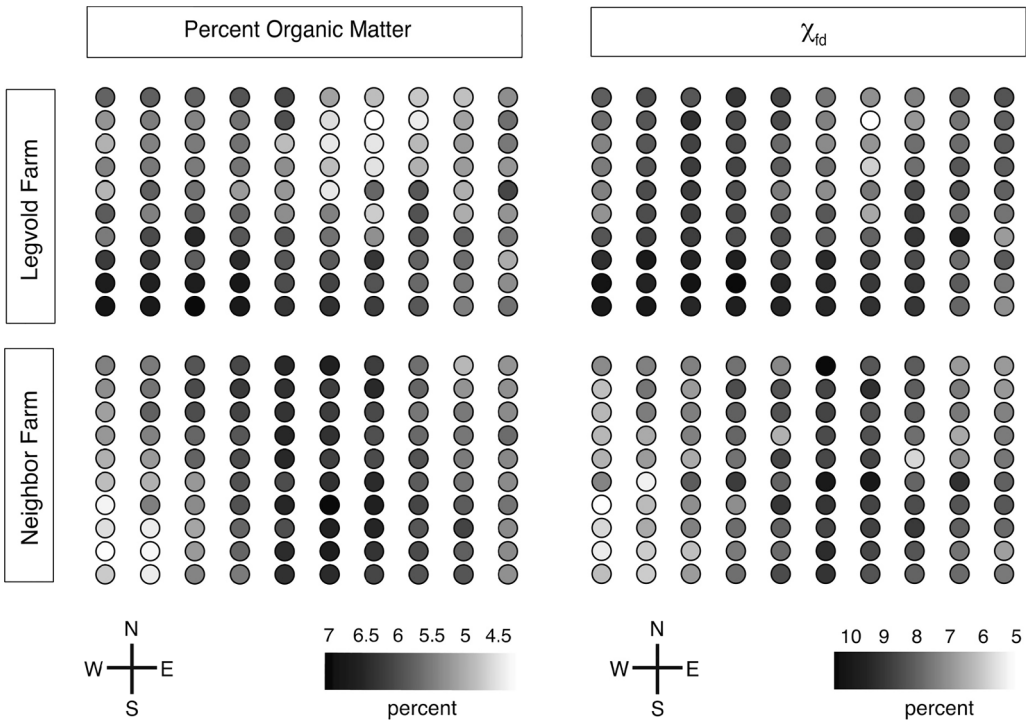

Fig. 2. Spatial variation of SOM and the frequency dependence of magnetic susceptibility (χ_{fd}; abundance of SP magnetite) in topsoil samples from a depth of 10–25 cm on the Legvold Farm and Neighbor Farm. The gradient scale denotes higher SOM and χ_{fd} with darker colors and lower SOM and χ_{fd} with lighter colors. Spaces between samples on W-E axis is 4 m, while spaces between samples on N-S axis is 2 m.

diamagnetic (weakly negative χ; for example, calcium carbonate), paramagnetic (weakly positive χ; for example, clay minerals), antiferromagnetic (positive χ; for example, hematite and goethite), and ferrimagnetic (strongly positive χ; for example, magnetite and maghemite) minerals. Ferrimagnetic minerals have χ values that are 2–3 orders of magnitude stronger than other mineral constituents and their contributions tend to dominate the soil χ signal when present, except in the case of clay-rich soils (Dearing et al., 1996; Dekkers, 1989; Jordanova and Jordanova, 1999; Maher, 2007; Yamazaki and Ioka, 1997). Accordingly, the χ of soils is often used as a rough proxy for the concentration of ferrimagnetic minerals present in a soil regardless of grain size or composition.

There are important behavioral changes in magnetic properties of ferrimagnetic minerals in soils that relate to grain size. In particular, fine-grained ferrimagnetic minerals (<30 nm for magnetite; Butler and Banerjee, 1975; Dunlop, 1973) behave as superparamagnetic (SP) materials that have a χ response that is sensitive to the frequency of the applied magnetic field (Dearing et al., 1996). At low-frequency (~465 Hz), nearly all of the SP grains in a sample will become dynamically aligned with the alternating field and contribute strongly to the measured χ. In contrast, at high frequencies, (~4650 Hz) the period of the alternating field is shorter than the relaxation time for SP particles and they are unable to fully align with the alternating field, and their contribution to the in-phase χ is reduced (Dearing et al., 1996; Dunlop and Özdemir, 2001; Maher, 2007; Thompson and Oldfield, 1986). It is possible, then, to quantify the contribution of SP grains to soil χ by investigating the frequency dependence of susceptibility (Dearing et al., 1996), a property that is widely applied in various environmental magnetic applications (Evans and Heller, 2003; Liu et al., 2012; Maher, 2007).

The frequency dependence of susceptibility is expressed in terms of either an absolute change, where $\chi_{fd} = \chi_{465\ Hz} - \chi_{4650\ Hz}$ with units of m^3kg^{-1}, or relative change where χ_{fd} is expressed as a percentage of the low-frequency χ ($\chi_{fd} = [(\chi_{465\ Hz} - \chi_{4650\ Hz}) / \chi_{465\ Hz}] \times 100$) (Dearing et al., 1996). Absolute χ_{fd} represents the concentration of SP grains while χ_{fd} expressed as a percentage represents the relative contribution of SP grains to the bulk low-frequency χ. In soils, a relative χ_{fd} of ~6% indicates abundant SP ferrimagnetic particles while values approaching the maximum theoretical values of ~15% indicate a soil with χ that is dominated by SP grains (Dearing et al., 1996). We note here that χ_{fd} alone does not definitively identify any particular ferrimagnetic iron oxide mineral, but in many soils, including some Minnesota soils (e.g., Maxbauer et al., 2017), χ_{fd} is almost always related to the abundance of SP magnetite and/or maghemite (γ-Fe_2O_3). Here, we report both absolute and relative χ_{fd} (identifiable by units of m^3kg^{-1} and percent, respectively), but refer to χ_{fd} as a singular property related to the abundance of SP magnetite throughout the discussion.

To better characterize the magnetic properties of topsoil in this study, including those related to a larger range of grain sizes, we selected a set of topsoil samples that represent the full range of χ_{fd} from each field (n = 30; the five highest, five lowest, and five closest to the median relative χ_{fd} from each field). These subset samples first acquired an anhysteretic remanent magnetization (ARM, Am^2kg^{-1}) in a peak alternating field (AF) of 100 mT with a weak direct current (DC) bias field of 50 μT. Subsequently, isothermal remanent magnetization (IRM, Am^2kg^{-1}) was imparted using three pulses of a 100 mT DC field with a pulse magnetizer. Remanence was measured immediately following acquisition using a 2G Enterprises 760-R SQUID magnetometer in a shielded room with a background magnetic field of less than 100 nT.

Both ARM and IRM are laboratory-applied remanent magnetizations that, by definition, can only be carried by ferrimagnetic or antiferromagnetic (together referred to as ferromagnetic) material with grain sizes that exceed the threshold for SP behavior (>30 nm for magnetite). At the field strengths applied here (100 mT) for ARM and IRM, we expect only grains of ferrimagnetic minerals to be contributing to these low field remanences (antiferromagnets generally require magnetic fields >100 mT to acquire remanence). Despite their importance in contributing to χ, SP grains are small enough that the thermal energy at room temperature acts to randomize any magnetic alignment in the absence of an applied field. However, as particle size increases, magnetic

minerals are able to retain a stable, uniform magnetization that characterizes stable, single domain (SD) behavior (30–75 nm grain size for magnetite; Dunlop, 1973; Butler and Banerjee, 1975). For even larger particles (grain sizes exceeding 300 nm) it become energetically favorable for grains to begin compartmentalizing magnetization into so-called 'domains', and these particles are referred to as multi-domain (MD). Magnetic particles with grain sizes that lie between SD and MD have variable magnetic behavior and are referred to as pseudo-single domain (PSD) grains (Dunlop, 1986; Roberts et al., 2017). Notably, pedogenic magnetic minerals tend to be in the SP-SD grain size range (Maher, 1998; Orgeira et al., 2011) while detrital grains are often coarser PSD-MD particles. The strength of a sample's IRM is dependent on the overall concentration of all ferromagnetic material present, generally independent of grain size. ARM in contrast is most effectively held by SD grains of magnetite and/or maghemite (Maher, 1988) and is frequently applied as a proxy for the concentration of SD magnetite in soils (e.g., Geiss et al., 2008). It is common in environmental magnetism to correct for variations in ARM that are due to concentration of magnetic minerals by normalizing ARM to IRM and reporting the ARM/IRM ratio (Geiss et al., 2008; Liu et al., 2012). Here, we interpret increases in ARM and ARM/IRM to be related to increases in the concentration and relative contributions to remanence of SD magnetite/maghemite, which is likely to be pedogenic.

Following low-field ARM and IRM acquisitions, a set of hysteresis loops and backfield remanence curves were measured for all subset samples using a Princeton Measurements Corporation MicroMag Vibrating Sample Magnetometer (VSM) at room temperature with a saturating fields of 1 Tesla. Commonly reported properties, including saturation magnetization (M_s, Am^2kg^{-1}), saturation remanent magnetization (M_{rs}, Am^2kg^{-1}), coercivity (B_c, mT), and the coercivity of remanence (B_{cr}, mT), are derived from hysteresis and backfield remanence measurements (see Tauxe et al., 2010).

All magnetic measurements for this study were conducted at the Institute for Rock Magnetism (IRM) at the University of Minnesota.

Differences in selected properties between the two fields were evaluated using the Welch two sample *t*-test for normally distributed data sets, while the nonparametric Mann-Whitney *U* test was applied to all data sets to provide a complete comparison of significance.

3. Results

3.1. Topsoil plots

Here we identify the most relevant measurements for our discussion (see Table 1 for summary data; full dataset available in supplementary material). Overall, the topsoil SOM in this study ranges from 4.5 to 7.2% with an average of 5.8 ± 0.6%. Both fields have broadly similar SOM values; however there are statistically significant differences between the SOM distributions from each field. In the Legvold field, SOM of topsoils ranges from 4.5 to 6.9% with an average of 5.7 ± 0.54% (see Table 1 for all summary data described here; full dataset available in supplementary material). The Neighbor field SOM values are significantly higher (p-value = 2.0×10^{-4} for a Welch two sample *t*-test; W = 3401, p-value = 9.3×10^{-5} for a Mann-Whitney *U* test), and range from 4.5 to 7.2% with an average of 6.0 ± 0.6%. We note that SOM exhibits spatial trend patterns on both plots (Fig. 2). In the Legvold field, higher SOM samples are located on the western and southern portions, with lower SOM samples mainly in the north to northeast areas. In the Neighbor field, many of the high SOM samples are located along a north–south transect in the center of the plot.

Magnetic susceptibility ($\chi_{465\ Hz}$) in this study ranges between 88.1 and 145.6 × 10^{-8} m^3kg^{-1} with an average of 120.9 ± 10.9 × 10^{-8} m^3kg^{-1}. These data sets were determined to be not normally distributed. Susceptibility is significantly lower (W = 9877, p-value = 2.2×10^{-16} for a Mann-Whitney *U* test) in Legvold topsoil (range 88.1 – 124.3 × 10^{-8} m^3kg^{-1}, average 111.9 ± 6.1 × 10^{-8} m^3kg^{-1}) compared with topsoil in the Neighbor field (range 112.8 – 145.6 × 10^{-8} m^3kg^{-1}, average 129.9 ± 6.2 × 10^{-8} m^3kg^{-1}).

The absolute frequency dependence of susceptibility (χ_{fd}) in topsoil from both fields in this study ranges from 2.4 to 14.1 × 10^{-8} m^3kg^{-1} with an average of 9.0 ± 2.0 × 10^{-8} m^3kg^{-1}. Legvold χ_{fd} ranges from 2.4 to 11.1 × 10^{-8} m^3kg^{-1} with an average of 7.8 ± 1.5 × 10^{-8} m^3kg^{-1}. The Neighbor field has absolute χ_{fd} values that vary between 6.9 and 14.1 × 10^{-8} m^3kg^{-1} with an average of 10.3 ± 1.5 × 10^{-8} m^3kg^{-1} and are significantly higher (p-value = 2.2×10^{-16} for a Welch two sample *t*-test; W = 8747, p-value = 2.2×10^{-16} for a Mann-Whitney *U* test). Relative χ_{fd} percentages range from 2.5 to 10.6% in the study and average 7.4 ± 1.2%. Values in the Legvold field (2.5–9.6%, average 6.9 ± 1.2%) are significantly lower (p-value = 8.3×10^{-9} for a Welch two sample *t*-test; W = 7295, p-value = 2.1×10^{-8} for a Mann-Whitney *U* test) than the Neighbor field (5.3–10.6%, average 7.9 ± 1.0%). The spatial variation for χ_{fd} matches variation of SOM in both fields, with higher χ_{fd} areas matching closely with areas of higher SOM values (and a similar relationship of low χ_{fd} and SOM values; Fig. 2).

Subset samples (n = 30) evaluated for remanence and hysteresis properties display trends similar to those observed in magnetic susceptibility, where Neighbor field topsoil skew towards slightly stronger magnetic properties compared to Legvold field topsoil.

We primarily report hysteresis and backfield remanent properties for topsoil subset samples as a means to constrain any variability in this study that might relate to changing mineralogy, and not simply a change in the concentration of the ferrimagnetic component (soil-formed magnetite/maghemite). Fig. 3 shows hysteresis loops (panel A) and a plot of the M_r/M_s vs. B_{cr}/B_c ratios – referred to commonly in the rock magnetic community as a Day Plot (Dunlop, 2002). Full results for hysteresis properties are available in the supplementary material. For simplicity, we limit our description of these data to emphasize two points. First, the consistency of the hysteresis loops shown in Fig. 3A and the low coercivities ($B_c < 10$ mT; $B_{cr} < 40$ mT) emphasize that there are minimal if any contributions of antiferromagnetic iron oxides (hematite or goethite). Second, our hysteresis data fall primarily along a mixing line in the Day Plot that highlights the finding that high SOM samples have a greater proportion of SD magnetite/maghemite, likely pedogenic (Fig. 3B).

Correlations between SOM and magnetic properties are reported in Table 2 and plotted in Fig. 4. Results from both farm fields display strong, positive, and significant correlations between SOM and χ_{fd} (absolute and relative), ARM, and ARM/IRM. Correlation between SOM and frequency dependence of susceptibility (a measure of SP magnetite/maghemite) is stronger in the Neighbor field compared with the Legvold

Table 1
Range, mean, and standard deviation (SD) of major magnetic properties and SOM.

Variable	Field	Range	Mean	SD
Topsoil SOM (%)	Legvold (n = 100)	4.5–6.9	5.7	0.54
	Neighbor (n = 100)	4.5–7.2	6.0	0.6
	All Samples (n = 200)	4.5–7.2	5.8	0.6
$\chi_{465\ Hz}$ (m^3kg^{-1}; x10^{-8})	Legvold	88.1–124.3	111.9	6.1
	Neighbor	112.8–145.6	129.9	6.2
	All Samples	88.1–145.6	120.9	10.9
Absolute χ_{fd} (m^3kg^{-1}; x10^{-8})	Legvold	2.4–11.1	7.8	1.5
	Neighbor	6.9–14.1	10.3	1.5
	All Samples	2.4–14.1	9.0	2.0
Relative χ_{fd} (%)	Legvold	2.5–9.6	6.9	1.2
	Neighbor	5.3–10.6	7.9	1.0
	All Samples	2.5–10.6	7.4	1.2
ARM (Am^2kg^{-1}; x10^{-4})	Legvold (n = 15)	0.9–2.7	2.1	0.6
	Neighbor (n = 15)	2.0–3.2	2.6	0.4
IRM (Am^2kg^{-1}; x10^{-3})	Legvold (n = 15)	4.9–8.0	6.0	0.9
	Neighbor (n = 15)	6.1–7.6	6.8	0.4
ARM/IRM (x10^{-2})	Legvold (n = 15)	1.4–5.2	3.6	1.1
	Neighbor (n = 15)	2.7–4.4	3.8	0.5

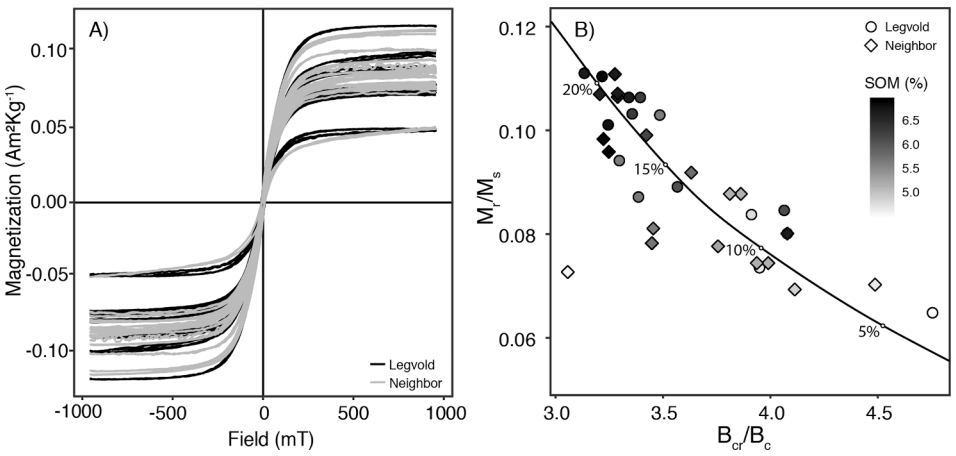

Fig. 3. A) Magnetic hysteresis of subset samples. All samples from both fields have relatively similar hysteresis properties, demonstrating similar minerology in each of the samples. B) Day plot of subset samples. Most data fall along the labeled mixing line between SD-MD magnetite where samples in the upper left-hand corner have a higher (~20%) proportion of SD magnetite and samples in the lower-right hand corner have a lower proportion (~5%) of SD magnetite (mixing line from Dunlop, 2002). Shading of symbols in panel B related to weight percent SOM and symbols refer to Legvold (circles) and Neighbor (diamonds) fields.

Table 2
Results from least-squares regressions between magnetic measurements and SOM. The coefficient of determination (r^2) quantifies the explanatory strength of magnetic properties in accounting for SOM variability (r^2 of 1 implies that a magnetic property can predict 100% of variability in SOM). The correlation (r) indicates the strength of the relationship between the two sets of data (r of 1 implies a perfect correlation between a magnetic property and SOM). The root mean square error (RMSE) provides a measure for model error. All regression models reported here are statistically significant at the $p < 0.001$ level.

Variables	Field	r^2	r	RMSE
χ_{fd} (relative) and SOM	Legvold	0.69	0.83	1.07
	Neighbor	0.88	0.94	0.83
	Legvold Vertical	0.67	0.81	1.09
	Neighbor Vertical	0.89	0.94	0.89
χ_{fd} (absolute) and SOM	Legvold	0.68	0.82	1.48×10^{-8}
	Neighbor	0.84	0.92	1.13×10^{-8}
ARM and SOM	Legvold	0.95	0.97	0.19
	Neighbor	0.81	0.90	0.37
ARM/IRM and SOM	Legvold	0.84	0.92	0.35
	Neighbor	0.50	0.71	0.60
χ_{fd} (relative) and ARM/IRM	Legvold	0.62	0.79	1.18
	Neighbor	0.59	0.77	1.53
χ_{fd} (absolute) and ARM/IRM	Legvold	0.67	0.82	1.50×10^{-8}
	Neighbor	0.70	0.84	1.57×10^{-8}

field (Table 2; Fig. 4, Panels A&B). In contrast, ARM and ARM/IRM (both measures of SD magnetite/maghemite) have stronger correlations with SOM in the Legvold field (Table 2; Fig. 4, Panels C&D). There is some variability in the slope of regressions between fields, most notably in the SOM-ARM and SOM-ARM/IRM regressions in Fig. 4C and 4D. Finally, there are also strong positive correlations among χ_{fd} (absolute and relative), ARM, and ARM/IRM (Table 2; Fig. S4).

3.2. Vertical profiles

Soil samples from vertical profiles (soil cores) in this study demonstrate similar positive correlation between χ_{fd} and SOM as those observed in topsoil samples (Fig. 5). Both χ_{fd} and SOM are relatively consistent from 10 to 30 cm depths due to vertical homogenization within the Ap horizon as a result of agricultural cultivation and plowing. Additionally, the relationship between χ_{fd} and SOM remains relatively consistent below 30 cm depth. The vertical profiles demonstrate strong, positive, and significant correlations between χ_{fd} and SOM, consistent with the topsoil samples in both fields (Fig. 6). Similar to topsoil samples, stronger correlations exist between χ_{fd} and SOM on the Neighbor field than the Legvold Farm (Table 2; Fig. 6). ARM and ARM/IRM were not evaluated on vertical profile samples.

SOM in samples from vertical profiles on the Legvold Farm range between 1.6 and 5.6% with an average of 3.4 ± 1.3%. On the Neighbor Farm, SOM ranges between 2.9 and 5.7% with an average of 4.35 ±1.1%. Relative χ_{fd} ranges between 0.7 and 8.0% with an average of 3.2 ± 2.52% on the Legvold Farm. On the Neighbor Farm, relative χ_{fd} ranges between 1.5 and 7.7% with an average of 5.93 ± 1.9%.

4. Discussion

The association between SOM and magnetic properties for agricultural soils reported here contributes to a small, but growing body of recent work emphasizing the utility of soil magnetism in agriculture and land management (Pingguo et al., 2016; Yang et al., 2015). To our knowledge, this study is the first to emphasize the strong association between SOM and magnetic properties in agricultural soils in North America. Positive correlations between soil magnetic properties and SOM (or organic carbon) are well documented across the world in a diverse set of non-agricultural soils including sites in the United Kingdom (Blundell et al., 2009b; Maher, 1998), Brazil (César de Mello et al., 2020), the Czech Republic (Jakšík et al., 2016), Bulgaria (Jordanova, 2016), Germany (Neumeister and Peschel, 1968), and Spain (Quijano et al., 2014). Here, we report positive correlations between magnetic properties (absolute and relative χ_{fd}; ARM and ARM/IRM) and SOM (Tables 1 and 2) that suggest an association between increased SOM and a greater abundance of pedogenically produced, fine-grained (SP/SD) magnetite and/or maghemite (referred to throughout the discussion simply as pedogenic magnetite). Below, we first discuss the observed variation in SOM and magnetic properties between the two study fields, describe the relationships between SOM and various magnetic measurements, and then conclude by describing a mechanistic basis for these relationships.

We expected a larger difference in SOM (and thus magnetic properties) between the Legvold field and Neighbor field due to differences in the recent land management practices. Many traditional agricultural practices (such as tillage) are well documented to reduce SOM over time through soil aggregate destruction, increased SOM oxidation, and erosion (Balesdent et al., 2000; Six et al., 1999). Given the adoption of sustainable land management practices at the Legvold Farm since the early 1990s (winter cover crops and strip tillage), we expected higher SOM values at the Legvold field. However, SOM in both fields is similar (ranges between 4.5% and 7.2%; see Fig. 4), and the average Neighbor field SOM is actually significantly higher than the Legvold field (p-value $= 2.0 \times 10^{-4}$ for a Welch two sample *t*-test). Studies of agricultural fields show that SOM recovery rates after long periods of conventional agriculture are irregular and complicated by soil textures and fertilizer use (Francis and Knight, 1993; Khorramdel et al., 2013; Stagnari et al., 2019). Perhaps, the lower SOM values in the Legvold field are explained by the ~50 year longer cultivation history of the Legvold field compared to the Neighbor field (although this interpretation remains speculative

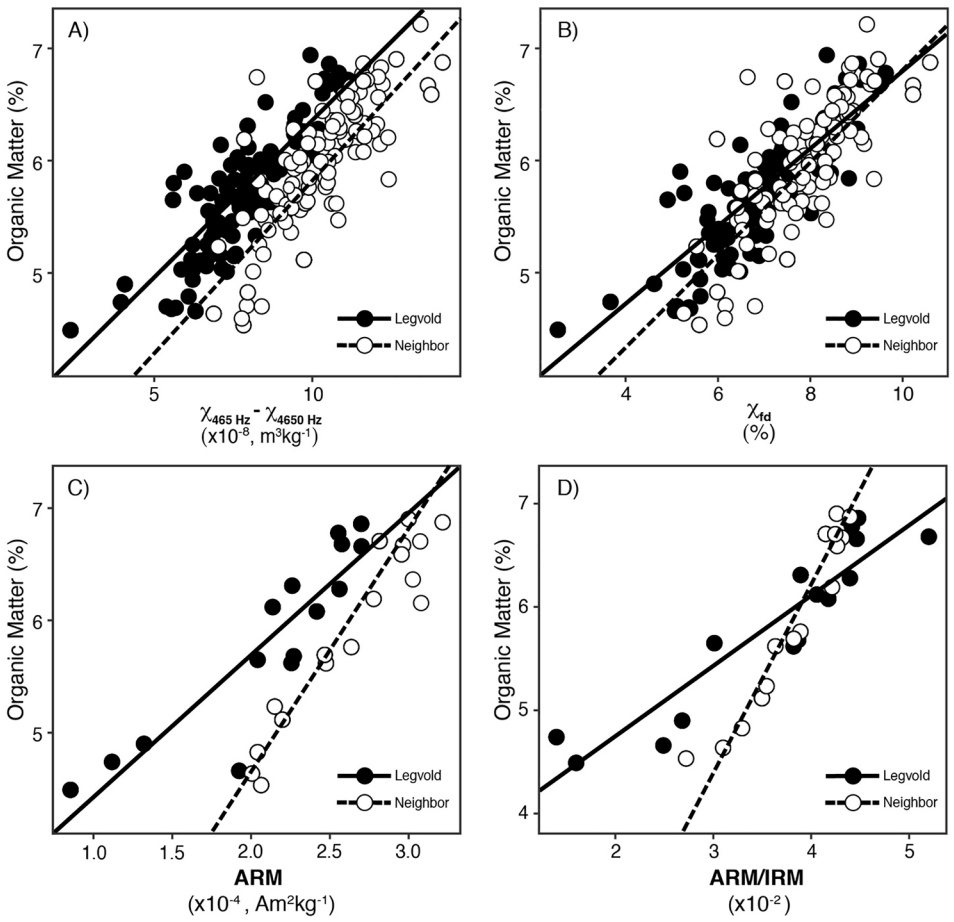

Fig. 4. Correlations between SOM and various magnetic properties on both the Legvold and Neighbor Farms. A) correlation between SOM and absolute frequency dependence of magnetic susceptibility (χ_{fd}). B) correlation between SOM and relative χ_{fd}. Increases in relative and absolute χ_{fd} represent an increase in concentration of SP (superparamagnetic) grains. C) correlation between SOM and ARM (anhysteretic remanent magnetization). D) correlation between SOM and ARM/IRM (ratio of anhysteretic remanent magnetization to isothermal remanent magnetization). Increases in both ARM and ARM/IRM are interpreted as increases in concentrations and contributions to remanence of SD (single domain) magnetite and/or maghemite. Samples collected from the Legvold Farm are represented by closed circle and a solid best-fit line. Samples collected from the Neighbor Farm are represented by open circles and a dashed best-fit line.

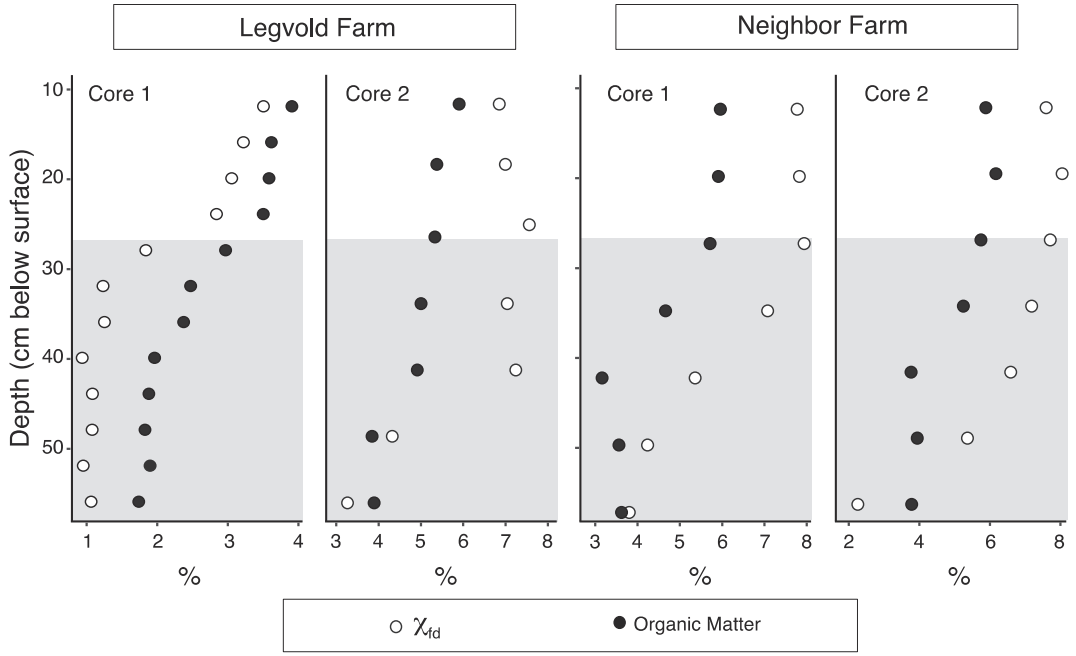

Fig. 5. Relative frequency dependence of magnetic susceptibility (χ_{fd}) and SOM measurements of four soil cores (vertical profiles), two collected from the Legvold Farm and two from the Neighbor Farm. Both χ_{fd} and SOM generally decrease below the plow depth in both fields, shown by the shaded region in each core. Note different scale on x-axis in the four plots.

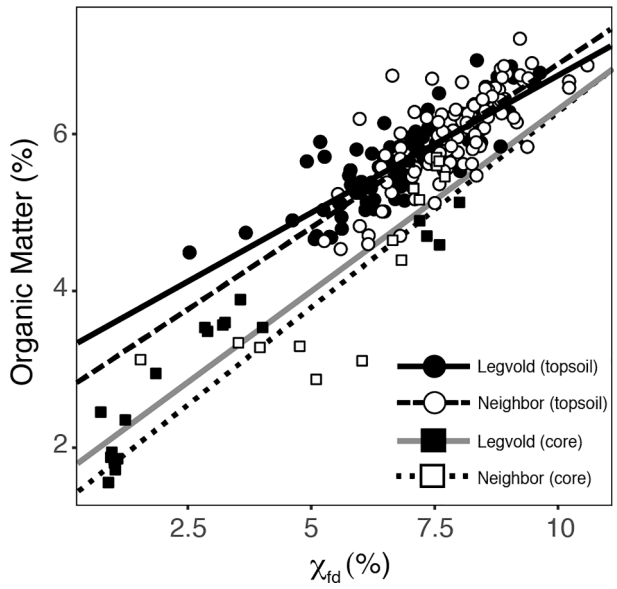

Fig. 6. Correlations between SOM and relative frequency dependence of magnetic susceptibility (χ_{fd}) for all soil samples (topsoil and core). Note the similar slopes among all four sets, indicating similar relationships between SOM and χ_{fd} at and below the ground surface. Core samples from the Legvold Farm are represented by closed squares and a gray best-fit line. Core samples from the Neighbor Farm are represented by open squares and a dashed best-fit line.

since historical data from these fields are not available to assess baseline conditions). Or, a more likely explanation may be that SOM has been depleted due to the use of artificial subsurface drainage (drain tiling) on the Legvold field, which generally decreases SOM stocks (Abid and Lal, 2008; Kumar et al., 2014). If so, artificial drainage may offset increases in SOM due to conservation practices, such as reduced tillage and cover crops. Our comparison of SOM between fields, then, supports the idea that long-term land use history (a century of cultivation) has a strong influence for establishing baseline soil properties, and that spatial patterns in SOM evolve over relatively long time periods. Notably, this implies any mechanistic linkage between SOM and magnetic properties ought to be responsive on similar timescales.

Within each field, there is a strong positive correlation between SOM and pedogenic magnetite (represented by absolute and relative χ_{fd}, ARM, and ARM/IRM) both in topsoil and at depth to at least 60 cm (Fig. 5, Fig. 6; Tables 1 and 2). Similar to patterns observed between fields with respect to SOM, grain-size dependent magnetic properties are significantly elevated in the Neighbor field compared with the Legvold field. Slopes of comparable regressions (and the strength of the correlations) differ slightly between the two fields and this may reflect the influence of confounding factors such as varying cultivation history or drainage patterns (artificially vs. naturally) in the two fields. For example, the difference in the regression of grain-size dependent properties against SOM (e.g., Fig. 4) may suggest the populations of SP and SD magnetite in these soils respond differently over time to variation in soil conditions – however, our data do not enable us to speculate on specific grain-size dependent properties beyond our discussion below. In general, we interpret these data to suggest that there is at least some mechanistic basis for the association between SOM and pedogenic magnetite (including SD and SP grainsizes together) observed in this study.

Pedogenic formation of magnetite in soils is well-known to be related to redox oscillations within soils during wet/dry cycles (see Fig. 7; Ahmed and Maher, 2018; Le Borgne, 1955; Le Borgne 1960; Mullins, 1977; Maher, 1998; Orgeira et al., 2011). A general description of this model begins with a consideration of wet (saturated) periods in soil, where soil pore waters become anoxic as aerobic respiration consumes available oxygen. With the onset of anoxia in soil porewater, anaerobic dissimilatory iron reducing bacteria (DIRB) activate and begin to reduce ferric iron in poorly crystalline oxyhydroxides (e.g., ferrihydrite) or other iron-bearing minerals (for example, siliciclastic clay minerals; see Hyodo et al., 2020) to ferrous iron through the oxidation of organic matter (Fig. 7; Kappler et al., 2004; Lovley and Phillips, 1986; Lovley et al., 1996, 1999; see Guyodo et al., 2006 for example of the difficulties in identifying precise role of bacteria in this process). Iron reduction, through the oxidation of SOM, contributes aqueous Fe^{2+} ions to soil porewater. During a drying phase, the reintroduction of oxygen leads to a mixed Fe^{2+}/Fe^{3+} solution that facilitates the precipitation of nanoscale magnetite (Fig. 7; Lovley, 1991; Lovley et al., 2004; Maher and Taylor, 1988; Orgeira et al., 2011; Taylor et al., 1987).

Given an adequate iron supply (which is easily achieved in most soils; see Orgeira et al., 2011), the pedogenic production of magnetite is

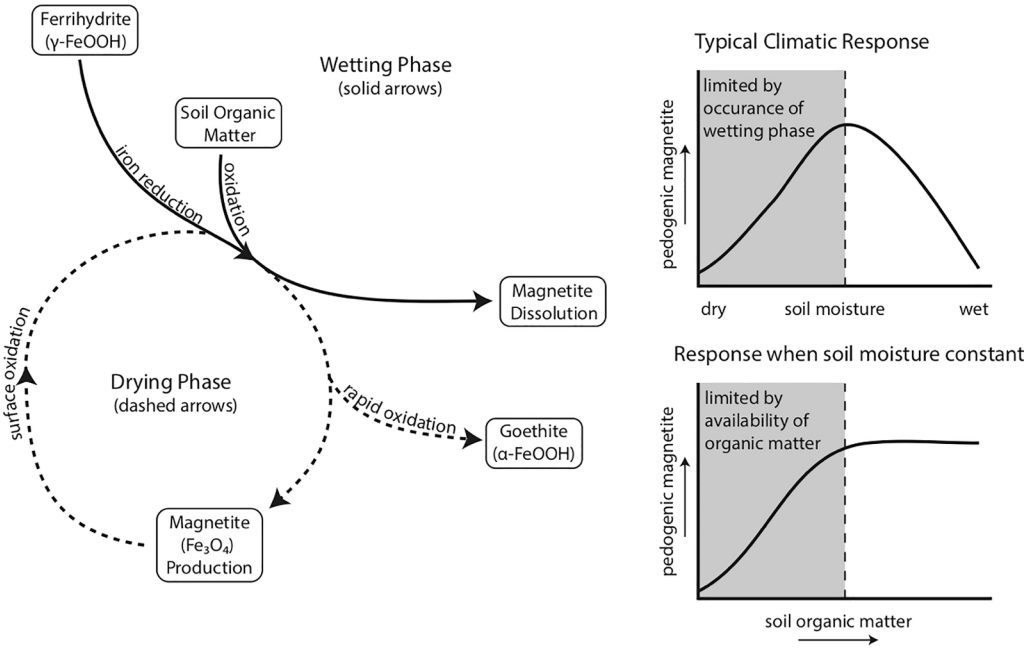

Fig. 7. Conceptual model relating redox dynamics during wet and dry phases of soil development, SOM oxidation, and magnetite formation (shown at left; conceptual model adapted from Orgeira et al., 2011). During wet periods, ferric iron from (oxy)hydroxide minerals (such as ferrihydrite) is reduced to Fe^{2+} through reaction with SOM serving an electron donor. During subsequent dry periods, nanoscale magnetite is precipitated (as one possible outcome; note goethite can also precipitate depending on soil conditions, see Bilardello et al. (2020) for recent example and discussion). Schematic graphs (at right) are meant to demonstrate the observed responses of pedogenic magnetite to climate/soil moisture (for example, see Balsam et al., 2011) and the expected relationship with soil organic matter.

typically thought to be limited by the occurrence and duration of anoxia during wet/dry cycles. Much of the literature on magnetic enhancement emphasizes the relationship between pedogenic magnetite and climate observed in well-drained soils where variation in soil moisture is related to precipitation (Fig. 7; Ahmed and Maher, 2018; Evans and Heller, 2003; Liu et al., 2012; Maher, 1998, 2007, 2011; Maxbauer et al., 2016; Orgeira et al., 2011; Thompson and Oldfield, 1986). These studies intentionally investigate soils that are relatively undisturbed and that occur across a regional climate gradient with variability in rainfall (typically between ~500 and 1500 mm yr^{-1}; reviewed in Maxbauer et al., 2016). In contrast, the agricultural soils in this study have relatively consistent soil moisture due to a combination of subsurface drainage (Legvold field), flat topography, similar soil types, and a consistent climate (rainfall, temperature, etc). In fact, most agricultural land is either naturally well-drained or artificially drained to improve production (see Blann et al., 2009 for history and statistics of drainage; Skaggs et al., 1994), to minimize variation in soil moisture across an individual field, and to aerate the soil profile. Therefore, the dominant role that climate and soil moisture play in dictating variation of pedogenic magnetite observed and studied in most modern soils does not apply to variations in pedogenic magnetite in a single agricultural field (although, they may for agricultural fields in different areas/regions).

SOM could be an alternative factor that limits the formation and accumulation of pedogenic magnetite in these settings through two possible pathways. First, SOM contributes the electrons necessary to reduce ferric iron in order to subsequently precipitate magnetite during dry phases. Second, nanoscale iron oxides (both poorly crystalline oxides like ferrihydrite along with other more crystalline oxides like magnetite) are known to stabilize soil organic matter and form iron-organic complexes within soil aggregates (Coward et al., 2017; Eusterhues et al., 2005; Inagaki et al., 2020; Wagai and Mayer, 2007; Zhao et al., 2016; Zhao et al., 2017). These iron-organic complexes may help facilitate the redox processes and subsequently lend stability to pedogenic magnetite in soils over time.

There ought to be considerable differences in the availability of SOM between comparable agricultural and undisturbed soils. For instance, conventional agricultural practices and artificial drainage reduce SOM levels in agricultural soils (Abid and Lal, 2008; Kumar et al., 2014), and most agricultural soils have relatively low SOM ranging from ~2 to 6% (with regional variance due to soil texture and climatic factors; Johnson et al., 2009). In a survey of soils from the United Kingdom, the strongest correlation between topsoil magnetic susceptibility and SOM was observed in settings where SOM was less than 9.4% (Blundell et al., 2009b; originally reported at soil organic carbon, converted here to SOM using a 1.74 conversion factor, see Pribyl, 2010; Nelson and Sommers, 1996). We suggest, then, that the magnetic properties of agricultural soils, where climate, drainage, and soil moisture are relatively consistent and SOM remains well below the threshold of 9.4% are ideally suited to show variation related to the availability of SOM (Fig. 7). Future work might address if the threshold identified by Blundell et al. (2009b) or SOM-magnetic correlations vary in different soil environments with other complicating factors (i.e. tropical soils with generally low cation-exchange capacity and arid soils with high calcium; Aprile and Lorandi 2012; Rowley et al., 2018). However, Blundell et al. (2009b)'s threshold is unlikely to be reached in most temperate agricultural settings.

An additional consideration regarding the relationship we discuss here is how sensitive soil magnetic properties and pedogenic magnetite production might be to changes in SOM. While the conversion of natural lands to agriculture results in a rapid loss of SOM (Post and Kwon, 2000), substantial changes in SOM on established agricultural lands tend to occur over relatively long time periods (several years to decades; Six et al., 2004; Zhang et al., 2016). If soil magnetism is to be a useful tool for soil characterization in agricultural systems, then pedogenic magnetite populations ought to occur in a state of equilibrium with respect to available SOM during pedogenesis (similar to equilibrium states of SOM and magnetic properties with respect to climate in undisturbed soils; see Maher, 1998; Maher, 2016). Several studies attempt to constrain the timescales required for magnetic enhancement to develop in non-agricultural soils (e.g., Fine et al., 1989; Lindquist et al., 2011; Maher et al., 2003; Quinton et al., 2011; Singer et al., 1992; Stinchcomb and Peppe, 2014; Vidic et al., 2004) and estimates range from $>10^4$ years to perhaps as quickly as a century (compare Fine et al., 1989; Singer et al., 1992 with Lindquist et al., 2011). Taken together, these studies support a slow (on human timescales), evolving equilibrium between soil conditions and pedogenic magnetite, similar to the long-term evolution of SOM (Maher, 2016).

The adapted mechanistic model we describe here agrees well with the observed correlations in our soils. In other comparable soils with glacial parent materials, or that are naturally or artificially well-drained, similar application of magnetism may prove to be a useful tool for agricultural soil surveys – however we note several important caveats. First, SOM-magnetic correlations are likely to be field specific (note variation in slope and regression coefficients for different fields in this study; Fig. 4 and Table 2) and field calibration (i.e. creating a training dataset of paired SOM-magnetic measurements) is required for any attempted application of these relationships. Second, the SOM-magnetic property relationships are likely to be variable in more diverse soil environments (i.e. tropical or non-glacial soils) or in areas with more diverse agricultural land management practices. Future studies that explore this relationship could aim to further develop soil magnetism as a tool for characterizing agricultural soil through investigations in more diverse settings.

5. Conclusions

In two agricultural fields near Northfield, Minnesota, SOM is positively and significantly correlated to four magnetic properties: absolute and relative χ_{fd}, ARM and ARM/IRM. Mechanistically, we suggest these correlations reflect SOM-limited pedogenic production of magnetite via microbial iron reduction in soils during wet/dry cycles. Given the relative consistency in soil moisture and low SOM in our study's agricultural soils, these conditions may be ideally suited to observe a correlation between SOM and soil magnetic properties. If these relationships are demonstrated in a wider variety of agricultural fields through further research, soil magnetism has potential to be utilized as a fairly rapid, low-cost method used for approximating SOM if calibrated at a field-scale. Continued work to better understand the relationship between soil magnetism and SOM in agricultural fields should aim to constrain other possible confounding factors (e.g., fields with greater topographic variation or varying soil texture) or associations with additional soil physical properties (e.g., cation exchange capacity; Maher, 1998). Our work here highlights the potential for magnetic measurements in evaluating SOM to develop as a tool for the agricultural community.

Declaration of Competing Interest

The authors declare that they have no known competing financial interests or personal relationships that could have appeared to influence the work reported in this paper.

Acknowledgements

This work was supported by the Frances and Rol Allensworth Endowed Fund of the Carleton College Geology Department. Thank you to David Legvold, the Legvold family, and the Volkert family for allowing us to conduct research in their fields. We thank the staff at the Institute for Rock Magnetism (IRM) and the National Lacustrine Core Facility (LacCore), especially Mike Jackson and Kristina Brady, at the University of Minnesota for allowing us to use their facilities to evaluate samples, and two anonymous reviewers for their helpful comments that improved this work.

Appendix A. Supplementary data

Supplementary data to this article can be found online at https://doi.org/10.1016/j.geoderma.2021.115466.

References

Abid, M., Lal, R., 2008. Tillage and drainage impact on soil quality. I. Aggregate stability, carbon and nitrogen pools. Soil Tillage Res. 100 (1–2), 89–98. https://doi.org/10.1016/j.still.2008.04.012.

Ahmed, I.A.M., Maher, B.A., 2018. Identification and paleoclimatic significance of magnetite nanoparticles in soils. Proc. Natl. Acad. Sci. U. S. A. 115 (8), 1736–1741. https://doi.org/10.1073/pnas.1719186115.

Aprile, F., Lorandi, R., 2012. Evaluation of cation exchange capacity (CEC) in tropical soils using four different analytical methods. J. Agric. Sci. 4, 278–289. https://doi.org/10.5539/jas.v4n6p278.

Balesdent, J., Chenu, C., Balabane, M., 2000. Relationship of soil organic matter dynamics to physical protection and tillage. Soil Tillage Res. 53 (3-4), 215–230. https://doi.org/10.1016/S0167-1987(99)00107-5.

Balsam, W.L., Ellwood, B.B., Ji, J., Williams, E.R., Long, X., El Hassani, A., 2011. Magnetic susceptibility as a proxy for rainfall: worldwide data from tropical and temperate climate. Quat. Sci. Rev. 30 (19-20), 2732–2744. https://doi.org/10.1016/j.quascirev.2011.06.002.

Bilardello, D., Banerjee, S.K., Volk, M.W.R., Soltis, J.A., Penn, R.L., 2020. Simulation of natural iron oxide alteration in soil: conversion of synthetic ferrihydrite to hematite without artificial dopants, observed with magnetic methods. Geochem. Geophys. Geosyst. 21, 1–19. https://doi.org/10.1029/2020GC009037.

Blann, K.L., Anderson, J.L., Sands, G.R., Vondracek, B., 2009. Effects of agricultural drainage on aquatic ecosystems: a review. Crit. Rev. Environ. Sci. Technol. 39 (11), 909–1001. https://doi.org/10.1080/10643380801977966.

Blundell, A., Hannam, J.A., Dearing, J.A., Boyle, J.F., 2009a. Detecting atmospheric pollution in surface soils using magnetic measurements: a reappraisal using an England and Wales database. Environ. Pollut. 157 (10), 2878–2890. https://doi.org/10.1016/j.envpol.2009.02.031.

Blundell, A., Dearing, J.A., Boyle, J.F., Hannam, J.A., 2009b. Controlling factors for the spatial variability of soil magnetic susceptibility across England and Wales. Earth-Science Rev. 95 (3-4), 158–188. https://doi.org/10.1016/j.earscirev.2009.05.001.

Butler, R.F., Banerjee, S.K., 1975. Theoretical single-domain grain size range in magnetite and titanomagnetite. J. Geophys. Res. 80 (29), 4049–4058. https://doi.org/10.1029/JB080i029p04049.

Camargo, L.A., Marques, J., Barrón, V., Alleoni, L.R.F., Pereira, G.T., Teixeira, D.D.B., de Bahia, A.S.R.S., 2018. Predicting potentially toxic elements in tropical soils from iron oxides, magnetic susceptibility and diffuse reflectance spectra. Catena 165, 503–515. https://doi.org/10.1016/j.catena.2018.02.030.

Cannell, R.Q., Hawes, J.D., 1994. Trends in tillage practices in relation to sustainable crop production with special reference to temperate climates. Soil Tillage Res. 30 (2-4), 245–282. https://doi.org/10.1016/0167-1987(94)90007-8.

César de Mello, D., Demattê, J.A.M., Silvero, N.E.Q., Di Raimo, L.A.D.L., Poppiel, R.R., Mello, F.A.O., Souza, A.B., Safanelli, J.L., Resende, M.E.B., Rizzo, R., 2020. Soil magnetic susceptibility and its relationship with naturally occurring processes and soil attributes in pedosphere, in a tropical environment. Geoderma 372, 114364. https://doi.org/10.1016/j.geoderma.2020.114364.

Coward, E.K., Thompson, A.T., Plante, A.F., 2017. Iron-mediated mineralogical control of organic matter accumulation in tropical soils. Geoderma 306, 206–216. https://doi.org/10.1016/j.geoderma.2017.07.026.

Dalal, R.C., Eberhard, R., Grantham, T., Mayer, D.G., 2003. Application of sustainability indicators, soil organic matter and electrical conductivity, to resource management in the northern grains region. Aust. J. Exp. Agric. 43, 253–259. https://doi.org/10.1071/EA00186.

Dean, W.E., 1974. Determination of carbonate and organic matter in calcareous sediments and sedimentary rocks by loss on ignition; comparison with other methods. J. Sediment. Petrology. 44, 242–248. https://doi.org/10.1306/74d729d2-2b21-11d7-8648000102c1865d.

Dearing, J.A., Dann, R.J.L., Hay, K., Lees, J.A., Loveland, P.J., Maher, B.A., O'Grady, K., 1996. Frequency-dependent susceptibility measurements of environmental materials. Geophys. J. Int. 124, 228–240. https://doi.org/10.1111/j.1365-246X.1996.tb06366.x.

Dekkers, M.J., 1989. Magnetic properties of natural goethite-I. Grain-size dependence of some low-and high-field related rockmagnetic parameters measured at room temperature. Geophys. J. Int. 97, 323–340. https://doi.org/10.1111/j.1365-246X.1989.tb00504.x.

Dunlop, D.J., 1973. Superparamagnetic and single-domain threshold sizes in magnetite. J. Geophys. Res. 78 (11), 1780–1793. https://doi.org/10.1029/JB078i011p01780.

Dunlop, D.J., 1986. Hysteresis properties of magnetite and their dependence on particle size: A test of pseudo-single-domain remanence models. J. Geophys. Res. 91, 9569–9584. https://doi.org/10.1029/jb091ib09p09569.

Dunlop, D.J., 2002. Theory and application of the Day plot (M_{rs} /M_s versus H_{cr} /H_c) 2. Application to data for rocks, sediments, and soils. J. Geophys. Res. 107, EPM5. https://doi.org/10.1029/2001jb000487.

Dunlop, D.J., Özdemir, O., 2001. Rock Magnetism: Fundamentals and Frontiers. Cambridge, United Kingdom.

Evans, M.E., Heller, F., 2003. Environmental Magnetism: Principles and Applications of Enviromagnetics. San Diego, California.

Eusterhues, K., Rumpel, C., Kögel-Knabner, I., 2005. Stabilization of soil organic matter isolated via oxidative degradation. Org. Geochem. 36 (11), 1567–1575. https://doi.org/10.1016/j.orggeochem.2005.06.010.

Fan, M., Lal, R., Zhang, H., Margenot, A.J., Wu, J., Wu, P., Zhang, L., Yao, J., Chen, F., Gao, C., 2020. Variability and determinants of soil organic matter under different land uses and soil types in eastern China. Soil Tillage Res. 198, 104544. https://doi.org/10.1016/j.still.2019.104544.

Ferreira, A.C.C., Leite, L.F.C., de Araújo, A.S.F., Eisenhauer, N., 2016. Land-use type effects on soil organic carbon and microbial properties in a semi-arid region of Northeast Brazil. L. Degrad. Dev. 27 (2), 171–178. https://doi.org/10.1002/ldr.2282.

Fine, P., Singer, M.J., La Ven, R., Verosub, K., Southard, R.J., 1989. Role of pedogenesis in distribution of magnetic susceptibility in two California chronosequences. Geoderma 44 (4), 287–306. https://doi.org/10.1016/0016-7061(89)90037-2.

Francis, G.S., Knight, T.L., 1993. Long-term effects of conventional and no-tillage on selected soil properties and crop yields in Canterbury. New Zealand. Soil Tillage Res. 26 (3), 193–210. https://doi.org/10.1016/0167-1987(93)90044-P.

Franzluebbers, A.J., 2002. Water infiltration and soil structure related to organic matter and its stratification with depth. Soil Tillage Res. 66 (2), 197–205. https://doi.org/10.1016/S0167-1987(02)00027-2.

Geiss, C.E., Egli, R., Zanner, C.W., 2008. Direct estimates of pedogenic magnetite as a tool to reconstruct past climates from buried soils. J. Geophys. Res. Solid Earth. 113, B11102. https://doi.org/10.1029/2008JB005669.

Gregory, M.M., Shea, K.L., Bakko, E.B., 2005. Comparing agroecosystems: effects of cropping and tillage patterns on soil, water, energy use and productivity. Renew. Agric. Food Syst. 20 (2), 81–90. https://doi.org/10.1079/RAF200493.

Guyodo, Y., LaPara, T.M., Anschutz, A.J., Penn, R.L., Banerjee, S.K., Geiss, C.E., Zanner, W., 2006. Rock magnetic, chemical and bacterial community analysis of a modern soil from Nebraska. Earth Planet. Sci. Lett. 251 (1-2), 168–178. https://doi.org/10.1016/j.epsl.2006.09.005.

Hanesch, M., Scholger, R., 2002. Mapping of heavy metal loadings in soils by means of magnetic susceptibility measurements. Environ. Geol. 42 (8), 857–870. https://doi.org/10.1007/s00254-002-0604-1.

Heiri, O., Lotter, A.F., Lemcke, G., 2001. Loss on ignition as a method for estimating organic and carbonate content in sediments: reproducibility and comparability of results. J. Paleolimnol. 25, 101–110. https://doi.org/10.1023/A:1008119611481.

Hobbs, H. C., Aronow, S. and Patterson, C. J., 1990. Surficial geology, pl. 3 of Balaban, N. H., and Hobbs, H. C., project managers, Geologic Atlas of Dakota County, Minnesota: Minnesota Geological Survey County Atlas C-6, pt. A, 9 pls., scale 1:100,000. https://conservancy.umn.edu/bitstream/handle/11299/58494/dakota_plt3_surficial%5b1%5d.pdf?sequence=9&isAllowed=y (accessed 1 August 2020).

Huang, B., Sun, W., Zhao, Y., Zhu, J., Yang, R., Zou, Z., Ding, F., Su, J., 2007. Temporal and spatial variability of soil organic matter and total nitrogen in an agricultural ecosystem as affected by farming practices. Geoderma 139 (3-4), 336–345. https://doi.org/10.1016/j.geoderma.2007.02.012.

Hyodo, M., Sano, T., Matsumoto, M., Seto, Y., Bradák, B., Suzuki, K., Fukuda, J., Shi, M., Yang, T., 2020. Nanosized authigenic magnetite and hematite particles in mature-paleosol phyllosilicates: new evidence for a magnetic enhancement mechanism in loess sequences of China. J. Geophys. Res. Solid Earth. 125, 1–25. https://doi.org/10.1029/2019JB018705.

Inagaki, T.M., Possinger, A.R., Grant, K.E., Schweizer, S.A., Mueller, C.W., Derry, L.A., Lehmann, J., Kögel-Knabner, I., 2020. Subsoil organo-mineral associations under contrasting climate conditions. Geochim. Cosmochim. Acta. 270, 244–263. https://doi.org/10.1016/j.gca.2019.11.030.

Jakšík, O., Kodešová, R., Kapička, A., Klement, A., Fér, M., Nikodem, A., 2016. Using magnetic susceptibility mapping for assessing soil degradation due to water erosion. Soil Water Res. 11 (No. 2), 105–113. https://doi.org/10.17221/233/2015-SWR.

Jordanova, N., 2016. Soil Magnetism: Applications in Pedology, Environmental Science, and Agriculture. Oxford, United Kingdom.

Jordanova, D., Jordanova, N., 1999. Magnetic characteristics of different soil types from Bulgaria. Stud. Geophys. Geod. 43, 303–318. https://doi.org/10.1023/A:1023398728538.

Jordanova, D., Jordanova, N., 2021. Updating the significance and paleoclimate implications of magnetic susceptibility of Holocene loessic soils. Geoderma 391, 1–17. https://doi.org/10.1016/j.geoderma.2021.114982.

Kappler, A., Benz, M., Schink, B., Brune, A., 2004. Electron shuttling via humic acids in microbial iron(III) reduction in a freshwater sediment. FEMS Microbiol. Ecol. 47, 85–92. https://doi.org/10.1016/S0168-6496(03)00245-9.

Khorramdel, S., Koocheki, A., Nassiri Mahallati, M., Khorasani, R., Ghorbani, R., 2013. Evaluation of carbon sequestration potential in corn fields with different management systems. Soil Tillage Res. 133, 25–31. https://doi.org/10.1016/j.still.2013.04.008.

Kumar, S., Nakajima, T., Mbonimpa, E.G., Gautam, S., Somireddy, U.R., Kadono, A., Lal, R., Chintala, R., Rafique, R., Fausey, N., 2014. Long-term tillage and drainage influences on soil organic carbon dynamics, aggregate stability and corn yield. Soil Sci. Plant Nutr. 60 (1), 108–118. https://doi.org/10.1080/00380768.2013.878643.

Larkin, R.P., 2015. Soil health paradigms and implications for disease management. Ann. Rev. Phytopathol. 53 (1), 199–221. https://doi.org/10.1146/annurev-phyto-080614-120357.

Le Borgne, E., 1955. Abnormal magnetic susceptibility of the topsoil. Ann. Geophys. 11, 399–419.

Le Borgne, E., 1960. Influence du feu sur les propriétés magnétiques du sol et sur celles du schiste et du granite. Ann. Geophys. 16, 159–195.

Lindquist, A.K., Feinberg, J.M., Waters, M.R., 2011. Rock magnetic properties of a soil developed on an alluvial deposit at Buttermilk Creek, Texas, USA. Geochemistry, Geophys. 12, 1–11. Geosystems. https://doi.org/10.1029/2011GC003848.

Liu, Q., Roberts, A.P., Larrasoaa, J.C., Banerjee, S.K., Guyodo, Y., Tauxe, L., Oldfield, F., 2012. Environmental magnetism: principles and applications. 50, RG4002. Rev. Geophys. https://doi.org/10.1029/2012RG000393.
Lovley, D.R., 1987. Organic matter mineralization with the reduction of ferric iron: a review. Geomicrobiol. J. 5 (3-4), 375–399. https://doi.org/10.1080/01490458709385975.
Lovley, D.R., 1991. Dissimilatory Fe(III) and Mn(IV) reduction. Microbiol. Rev. 2, 259–287. https://doi.org/10.1128/mmbr.55.2.259-287.1991.
Lovley, D.R., Phillips, E.J.P., 1986. Organic matter mineralization with reduction of ferric iron in anaerobic sediments. Appl. Environ. Microbiol. 51 (4), 683–689. https://doi.org/10.1128/aem.51.4.683-689.1986.
Lovley, D.R., Coates, J.D., Blunt-Harris, E.L., Phillips, E.J.P., Woodward, J.C., 1996. Humic substances as electron acceptors for microbial respiration. Nature 382 (6590), 445–448. https://doi.org/10.1038/382445a0.
Lovley, D.R., Fraga, J.L., Coates, J.D., Blunt-Harris, E.L., 1999. Humics as an electron donor for anaerobic respiration. Environ. Microbiol. 1 (1), 89–98. https://doi.org/10.1046/j.1462-2920.1999.00009.x.
Lovley, D.R., Holmes, D.E., Nevin, K.P., 2004. Dissimilatory Fe(III) and Mn(IV) reduction. Adv. Microb. Physiol. 49, 219–286. https://doi.org/10.1016/S0065-2911(04)49005-5.
Maher, B.A., 1988. Magnetic properties of some synthetic sub-micron magnetites. Geophys. J. 94 (1), 83–96. https://doi.org/10.1111/j.1365-246X.1988.tb03429.x.
Maher, B.A., 1998. Magnetic properties of modern soils and Quaternary loessic paleosols: paleoclimatic implications. Palaeogeogr. Palaeoclimatol. Palaeoecol. 137 (1-2), 25–54. https://doi.org/10.1016/S0031-0182(97)00103-X.
Maher, B.A., 2007. Environmental magnetism and climate change. Contemp. Phys. 48 (5), 247–274. https://doi.org/10.1080/00107510801889726.
Maher, B.A., 2011. The magnetic properties of Quaternary aeolian dusts and sediments, and their palaeoclimatic significance. Aeolian Res. 3 (2), 87–144. https://doi.org/10.1016/j.aeolia.2011.01.005.
Maher, B.A., 2016. Palaeoclimatic records of the loess/palaeosol sequences of the Chinese Loess Plateau. Quat. Sci. Rev. 154, 23–84. https://doi.org/10.1016/j.quascirev.2016.08.004.
Maher, B.A., MengYu, H., Roberts, H.M., Wintle, A.G., 2003. Holocene loess accumulation and soil development at the western edge of the Chinese Loess Plateau: implications for magnetic proxies of palaeorainfall. Quat. Sci. Rev. 22 (5-7), 445–451. https://doi.org/10.1016/S0277-3791(02)00188-9.
Maher, B.A., Taylor, R.M., 1988. Formation of ultrafine-grained magnetite in soils. Nature 336 (6197), 368–370. https://doi.org/10.1038/336368a0.
Marchetti, A., Piccini, C., Francaviglia, R., Mabit, L., 2012. Spatial distribution of soil organic matter using geostatistics: a key indicator to assess soil degradation status in central Italy. Pedosphere 22 (2), 230–242. https://doi.org/10.1016/S1002-0160(12)60010-1.
Maxbauer, D.P., Feinberg, J.M., Fox, D.L., 2016. Magnetic mineral assemblages in soils and paleosols as the basis for paleoprecipitation proxies: a review of magnetic methods and challenges. Earth-Science Rev. 155, 28–48. https://doi.org/10.1016/j.earscirev.2016.01.014.
Maxbauer, D.P., Feinberg, J.M., Fox, D.L., Nater, E.A., 2017. Response of pedogenic magnetite to changing vegetation in soils developed under uniform climate, topography, and parent material. Sci. Rep. 7, 1–10. https://doi.org/10.1038/s41598-017-17722-2.
Mullins, C.E., 1977. Magnetic susceptibility of the soil and its significance in soil science – a review. J. Soil Sci. 28, 223–246. https://doi.org/10.1111/j.1365-2389.1977.tb02232.x.
National Weather Service Forecast Office, National Oceanic and Atmospheric Administration, 2019. https://w2.weather.gov/climate/index.php?wfo=mpx (accessed 1 August 2020).
Nelson, D.W., Sommers, L.E., 1996. Total carbon, organic carbon, and organic matter. Methods of soil analysis: Part 2 chemical and microbiological properties 9, 539–579. https://doi.org/10.2136/sssabookser5.3.c34.
Neumeister, H., Peschel, G., 1968. Magnetic susceptibility of soils and Pleistocene sediments in the neighborhood of Leipzig. Albrecht-Thaer-Arch. 12, 1055–1072. https://doi.org/10.1080/03650346809412311.
Orgeira, M.J., Egli, R., Compagnucci, R.H., 2011. A quantitative model of magnetic enhancement in loessic soils. In: Petrovský, E., Herrero-Bervera, E., Harinarayana, T., Ivers, D. (Eds.), The Earth's Magnetic Interior. Springer, Netherlands, pp. 361–397. https://doi.org/10.1007/978-94-007-0323-0_25.
Pingguo, Y., Byrne, J.M., Yang, M., 2016. Spatial variability of soil magnetic susceptibility, organic carbon and total nitrogen from farmland in northern China. Catena 145, 92–98. https://doi.org/10.1016/j.catena.2016.05.025.
Post, W.M., Kwon, K.C., 2000. Soil carbon sequestration and land-use change: processes and potential. Glob. Chang. Biol. 6, 317–327. https://doi.org/10.1046/j.1365-2486.2000.00308.x.
Pribyl, D.W., 2010. A critical review of the conventional SOC to SOM conversion factor. Geoderma 156 (3-4), 75–83. https://doi.org/10.1016/j.geoderma.2010.02.003.
Quijano, L., Chaparro, M.A.E., Marie, D.C., Gaspar, L., Navas, A., 2014. Relevant magnetic and soil parameters as potential indicators of soil conservation status of Mediterranean agroecosystems. Geophys. J. Int. 198 (3), 1805–1817. https://doi.org/10.1093/gji/ggu239.
Quinton, E.E., Dahms, D.E., Geiss, C.E., 2011. Magnetic analyses of soils from the Wind River Range, Wyoming, constrain rates and pathways of magnetic enhancement for soils from semiarid climates. Geochem. Geophys. Geosystems. 12 (7), n/a–n/a. https://doi.org/10.1029/2011GC003728.
Rawls, W.J., Pachepsky, Y.A., Ritchie, J.C., Sobecki, T.M., Bloodworth, H., 2003. Effect of soil organic carbon on soil water retention. Geoderma 116 (1-2), 61–76. https://doi.org/10.1016/S0016-7061(03)00094-6.
Reeves, D.W., 1997. The role of soil organic matter in maintaining soil quality in continuous cropping systems. Soil Tillage Res. 43 (1-2), 131–167. https://doi.org/10.1016/S0167-1987(97)00038-X.
Roberts, A.P., Almeida, T.P., Church, N.S., Harrison, R.J., Heslop, D., Li, Y., Li, J., Muxworthy, A.R., Williams, W., Zhao, X., 2017. Resolving the origin of pseudo-single domain magnetic behavior. J. Geophys. Res. Solid Earth 122 (12), 9534–9558. https://doi.org/10.1002/jgrb.v122.1210.1002/2017JB014860.
Rowley, M.C., Grand, S., Verrecchia, É.P., 2018. Calcium-mediated stabilisation of soil organic carbon. Biogeochemistry 137 (1-2), 27–49. https://doi.org/10.1007/s10533-017-0410-1.
Santisteban, J.I., Mediavilla, R., López-Pamo, E., Dabrio, C.J., Blanca Ruiz Zapata, M., José Gil García, M., Castaño, S., Martínez-Alfaro, P.E., 2004. Loss on ignition: a qualitative or quantitative method for organic matter and carbonate mineral content in sediments? J. Paleolimnol. 32 (3), 287–299. https://doi.org/10.1023/B:JOPL.0000042999.30131.5b.
Singer, M.J., Fine, P., Verosub, K.L., Chadwick, O.A., 1992. Time dependence of magnetic susceptibility of soil chronosequences on the California coast. Quat. Res. 37 (3), 323–332. https://doi.org/10.1016/0033-5894(92)90070-Y.
Six, J., Elliott, E.T., Paustian, K., 1999. Aggregate and soil organic matter dynamics under conventional and no-tillage systems. Soil Sci. Soc. Am. J. 63 (5), 1350–1358. https://doi.org/10.2136/sssaj1999.6351350x.
Six, J., Ogle, S.M., Breidt, F.J., Conant, R.T., Mosiers, A.R., Paustian, K., 2004. The potential to mitigate global warming with no-tillage management is only realized when practised in the long term. Glob. Chang. Biol. 10, 155–160. https://doi.org/10.1111/j.1529-8817.2003.00730.x.
Skaggs, R.W., Brevé, M.A., Gilliam, J.W., 1994. Hydrologic and water quality impacts of agricultural drainage. Crit. Rev. Environ. Sci. Technol. 24 (1), 1–32. https://doi.org/10.1080/10643389409388459.
Soil Survey Staff, National Resources Conservation Service, United States Department of Agriculture, 2020. Web Soil Survey. https://websoilsurvey.sc.egov.usda.gov/ (accessed 1 August 2020).
Soil Survey Staff, National Resources Conservation Service, United States Department of Agriculture, 2006. Blooming Series. https://soilseries.sc.egov.usda.gov/OSD_Docs/B/BLOOMING.html (accessed 1 August 2020).
Soil Survey Staff, 2014, Soil Survey Field and Laboratory Methods Manual. Soil Survey Investigations Report No. 51. https://www.nrcs.usda.gov/Internet/FSE_DOCUMENTS/stelprdb1253871.pdf (accessed 1 August 2020).
Stagnari, F., Galieni, A., D'Egidio, S., Pagnani, G., Pisante, M., 2019. Sustainable soil management. In: Farooq, M., Pisante, M. (Eds.), Innovations in Sustainable Agriculture. Springer International Publishing, Cham, pp. 105–131.
Stinchcomb, G.E., Peppe, D.J., 2014. The influence of time on the magnetic properties of late Quaternary periglacial and alluvial surface and buried soils along the Delaware River, USA. Front. Earth Sci. 2, 1–14. https://doi.org/10.3389/feart.2014.00017.
Tauxe, L., Banerjee, S.K., Butler, R.F., van der Voo, R., 2010. Essentials of Paleomagnetism. California, Berkeley.
Taylor, R.M., Maher, B.A., Self, P.G., 1987. Magnetite in soils: I. The synthesis of single-domain and superparamagnetic magnetite. Clay Miner. 22 (4), 411–422. https://doi.org/10.1180/claymin.1987.022.4.05.
Thompson, R., Oldfield, F. (Eds.), 1986. Environmental Magnetism. Springer Netherlands, Dordrecht.
United States Department of Agriculture, 1983. Soil Survey of Dakota County Minnesota. https://www.blogs.nrcs.usda.gov/Internet/FSE_MANUSCRIPTS/minnesota/MN037/0/Dakota_MN.pdf (accessed 1 August 2020).
Vidic, N.J., Singer, M.J., Verosub, K.L., 2004. Duration dependence of magnetic susceptibility enhancement in the Chinese loess-palaeosols of the past 620 ky. Palaeogeogr. Palaeoclimatol. Palaeoecol. 211 (3-4), 271–288. https://doi.org/10.1016/j.palaeo.2004.05.012.
Wagai, R., Mayer, L.M., 2007. Sorptive stabilization of organic matter in soils by hydrous iron oxides. Geochim. Cosmochim. Acta. 71 (1), 25–35. https://doi.org/10.1016/j.gca.2006.08.047.
Yamazaki, T., Ioka, N., 1997. Environmental rock-magnetism of pelagic clay: implications for Asian eolian input to the North Pacific since the Pliocene. Paleoceanography 12 (1), 111–124. https://doi.org/10.1029/96PA02757.
Yang, P.G., Yang, M., Mao, R.Z., Byrne, J.M., 2015. Impact of long-term irrigation with treated sewage on soil magnetic susceptibility and organic matter content in North China. Bull. Environ. Contam. Toxicol. 95 (1), 102–107. https://doi.org/10.1007/s00128-015-1562-0.
Zhang, Z., Qiang, H., McHugh, A.D., He, J., Li, H., Wang, Q., Lu, Z., 2016. Effect of conservation farming practices on soil organic matter and stratification in a mono-cropping system of Northern China. Soil Tillage Res. 156, 173–181. https://doi.org/10.1016/j.still.2015.10.008.
Zhao, Q., Adhikari, D., Huang, R., Patel, A., Wang, X., Tang, Y., Obrist, D., Roden, E.E., Yang, Y., 2017. Coupled dynamics of iron and iron-bound organic carbon in forest soils during anaerobic reduction. Chem. Geol. 464, 118–126. https://doi.org/10.1016/j.chemgeo.2016.12.014.
Zhao, Q., Poulson, S.R., Obrist, D., Sumaila, S., Dynes, J.J., McBeth, J.M., Yang, Y., 2016. Iron-bound organic carbon in forest soils: quantification and characterization. Biogeosciences. 13 (16), 4777–4788. https://doi.org/10.5194/bg-13-4777-2016.